Finite-temperature effects on the stability and infrared spectra of $HCl(H_2O)_6$ clusters

U. F. T. Ndongmouo[1], M.-S. Lee[1,2], R. Rousseau[3], F. Baletto[1,4], S. Scandolo[1,5]

[1] *The Abdus Salam International Centre for Theoretical Physics, Trieste, I-34014 Italy*

[2] *Centre for modeling and simulation,*
and Department of Physics, University of Pune,
Ganeshkhind, Pune 411 007, India

[3] *International School For Advanced Studies (SISSA), Trieste, I-34014 Italy*

[4] *DMSE-MIT, 77 Massachusetts Ave., Cambridge MA 02139 USA*

[5] *INFM/CNR "Democritos" National Simulation Center, Trieste, Italy*

Abstract

Theoretical studies of the interaction of HCl with small water clusters have so far neglected the effect of temperature, which ranges from a few tens of Kelvin in cluster experiments, up to about 250 K in typical atmospheric conditions. We study the dynamical behavior of a selected set of $HCl(H_2O)_6$ clusters, representative of undissociated and dissociated configurations, by means of DFT-based first principles molecular dynamics. We find that the thermodynamical stability of different configurations can be affected by temperature. We also present the infrared spectra of dissociated and undissociated configurations at 200 K and discuss the origin of the spectral features.

I. INTRODUCTION

The molecular pathways leading to the dissociation of strong acids in/on water systems have been the subject of intense study in the last years. The HCl/water system is of particular interest due to the strong affinity of HCl for ice and to the possible implications that HCl dissociation may have in the heterogeneous chemistry of the atmosphere. Chlorine radicals activated at the ice surfaces of polar stratospheric cloud particles are believed to play an important role in atmospheric ozone depletion in polar regions [1–4]. Laboratory data leading to molecular descriptions of the reactions are sparse due to the difficulty of performing surface experiments on a high vapor pressure material such as ice [5]. As a consequence, the chemical pathway is not understood in details [6–8]. Two points are under a strong debate. One regards the uptake of a strong acid at the surface of ice; the other is related to the dynamics of the acid dissociation and the formation of active chlorine atoms [9]. Crucial to both aspects is a detailed understanding of the interaction of the acid with the surrounding shell of water molecules. In this context, efforts have focused either on extended systems such as monohydrate crystals and solutions [10, 11], or on small HCl-H_2O clusters [12–27]. HCl partial or complete dissociation in extended systems has been interpreted in terms of formation of H_3O^+ or $H_5O_2^+$, and Cl^- ions. Experimental studies on HCl-water clusters are hampered by difficulties in detecting clusters larger than $HCl(H_2O)_2$ [12], due to the stronger affinity of small water clusters for water than for HCl [13]. As a consequence, most of our understanding regarding HCl-water clusters comes from theoretical studies. Several molecular dynamics simulations and *ab initio* calculations have been performed to study the interaction of HCl with progressively larger water clusters, with the aim of identifying the crucial number of water molecules to dissociate the HCl molecule and add insight into the molecular mechanisms responsible for the dissociation. *Ab initio* molecular orbital studies show that the most stable configuration of the HCl-H_2O system is the hydrogen-bonded molecular complex, while the proton-transferred ionic structure is higher in energy [14, 15]. Proton transfer from HCl to water was predicted to be unfavorable also in HCl-water clusters with up to three water molecules [13, 16, 17]. Lee *et al.* have suggested an ionic structure for the ground state of clusters with four water molecules [18]. Re *et al.* found that proton transfer in the hydrogen-bonded cluster $HCl(H_2O)_n$ with $n = 1 - 5$ completely occurs only in the case of $n = 5$ clusters [19]. Using the B3LYP density functional method and

the CCSD(T) *ab initio* method, Milet *et al.* showed however that HCl starts dissociating already in $HCl(H_2O)_4$ [20]. Devlin *et al.*, using *ab initio* Monte Carlo simulations found that in $HCl(H_2O)_6$ three-coordinated HCl dissociates directly to form a clearly recognizable solvated Cl^- and H_3O^+ ion pair [21]. They also suggested that to induce ionization, HCl must bind to a two-coordinated dangling-O molecule, that is, one that does not accept a proton from another H_2O molecule.

Theoretical studies have so far neglected the possible effect of temperature in the dissociation process. Temperatures relevant to atmospheric processes range between 200 K and 250 K. Temperatures in clusters produced in the laboratory are less constrained, but are believed to be between 50 K to 200 K, depending on the experimental set-up. Temperature has certainly an important role in the dynamics of dissociation, but evidence is raising that temperature might also have an important role in determining the thermodynamical stability of different cluster forms. In the case of HBr, for example, experiment and theory disagree regarding the minimum number n of H_2O molecules required to dissociate the acid [28–30], with theory predicting a stable dissociated state already for $n = 4$ and laser spectroscopy on clusters showing that at least 5 molecules are required to dissociate HBr. Calculations being done at zero temperature, and experiments at finite temperatures, a possible reason for the discrepancy is the effect of temperature on the stability of different (dissociated or undissociated) forms [30]. In the case of HCl, *ab initio* free-energy calculations within the harmonic approximation suggest a destabilization of the dissociated state when temperature is raised from 0 to 300 K, in the case of $n = 4$ [31]. Temperature effects on the relative stability of different structures has been already considered in the case of *pure* water clusters. Theoretical studies find important changes as a function of temperature, with more open (cyclic) structures preferred at high temperature over compact structures [32, 33]. Temperature-induced structural changes may have important implications for the reactivity of the cluster and its capability to dissociate the acid.

Here, we focus our attention on the interaction of HCl with a water hexamer ($n = 6$) at the temperature conditions found in the lower troposphere (about 200 K), via density-functional-based first principles molecular dynamics. The choice of $HCl(H_2O)_6$ is motivated by the possibility to compare our findings with experimental results, which are available so far only for HCl on ice surfaces. Six-membered rings are the smallest topologically closed arrangements of H_2O molecules in ice and at its ideal surfaces, so $HCl(H_2O)_6$ can be seen as

representative of a typical molecular environment found by HCl adsorbed at the surface of ice. Starting from the analysis of the energetic properties of different $HCl(H_2O)_6$ isomers, we present the dynamical behavior of two configurations representative of a dissociated and of a non-dissociated system, respectively.

II. SIMULATION METHODS

Geometrical optimizations, energies, and infrared spectra of $HCl(H_2O)_6$ clusters were determined by means of density-functional theory (DFT) methods, with a gradient corrected exchange correlation functional (BLYP). The choice of the BLYP functional is supported by its accuracy in reproducing the results obtained with higher-level methods in pure water clusters [34]. Troullier-Martins pseudopotentials were adopted to describe valence electron-nuclei interactions [35]. Orbitals were expanded in a plane wave basis set with an energy cut-off of 80 Ry. This cutoff ensures convergence of the electronic states with respect to the plane wave basis set in the case of pure water, as already shown [36], and is therefore appropriate also for Cl, whose valence radius is larger than that of oxygen. In the plane wave approach, the system is repeated periodically in three dimensions. The simulation box size was found to be converged at 35 bohrs (19 Å). DFT plane-wave calculations were performed with the Quantum-Espresso package [37]. Relaxed structures were also optimized at the MP2/6-311G** level using Gaussian03 [38].

For the dynamical runs at finite temperature, electronic states and the atomic positions were evolved with the Car-Parrinello method [39]. The fictitious electronic mass μ was fixed to 250 a.u., with a time step of 0.12 fs (5 a.u.) for the integration of the equations of motions using the velocity-Verlet algorithm. Recent studies have highlighted the need to use a small electronic mass (smaller than one fifth of the lightest atomic mass in the system [40]) in order to ensure an adiabatic evolution of the electronic degrees of freedom on the Born-Oppenheimer surface, over the full length of the MD trajectory. Our value of $\mu = 250$ a.u. is about eight times smaller than the mass of the proton. Forces on atoms were computed using the Hellman-Feynman theorem and wave functions were assumed to have the periodicity of the simulation cell. The target temperature of 200 K was reached by heating up the system gradually with temperature steps of 40 K followed by equilibration for at least 4 ps at each temperature. At each temperature the trajectories were initially

thermalized for about ∼1.5 ps via a Nosé-Hoover thermostat, followed by a micro-canonical run of ∼ 2.5 ps. At 200 K the total simulation time was about 25 ps for each structure, and averages were taken during the last 20 ps.

Infrared (IR) spectra were calculated from the Fourier transform of the time self-correlation of the total dipole moment [41].

$$\alpha(\omega) = \frac{4\pi\omega \tanh(\beta\hbar\omega/2)}{3\hbar\, n\, c} \int_0^{+\infty} dt\, e^{-i\omega t} \langle \mathbf{M}(t) \cdot \mathbf{M}(0) \rangle, \quad (1)$$

where T is the temperature, $\beta = 1/(k_B T)$, n is the refractive index (in our case we take n=1), c is the speed of light in vacuum, $\mathbf{M}$ is the total dipole moment (including nuclear and electronic components) and the angular brackets indicate a statistical average over initial times. The electronic dipole moment at each time step was evaluated using a Berry-phase approach [41].

III. RESULTS AND DISCUSSIONS

A. Geometry configurations of HCl water clusters

The structure of $HCl(H_2O)_6$ clusters has not been investigated in experiments yet, and theoretical studies have only considered configurations representative of the local environment found at the surface of ice [21], including dissociated, undissociated, and partially dissociated structures, but have not addressed their energetic stability. The structures of pure $(H_2O)_6$ clusters have been instead studied more extensively. The lowest-energy configuration is still debated, with several isomers, so called book, cage, prism, and ring (also called cyclic) structures [42], displaying similar energies, at various levels of theory. Recent studies on the water hexamer [32, 33] have shown that the ring structure is likely to be the most stable at high temperature. In order to study the finite temperature properties of $HCl(H_2O)_6$ clusters by molecular dynamics, we start by constructing a set of representative initial configurations. Because the ring isomer is the lowest energy structure for the $(H_2O)_6$ cluster, according to our DFT-BLYP calculations, we started by constructing structures representative of the undissociated system by placing the HCl molecule in different positions along the ring isomer of the water hexamer. The ring isomer is not a good starting structure if the purpose is to construct a dissociated system, however. Earlier studies [19] have shown that a minimum of three hydrogen bonds is required for the dissociation of HCl. Thus,

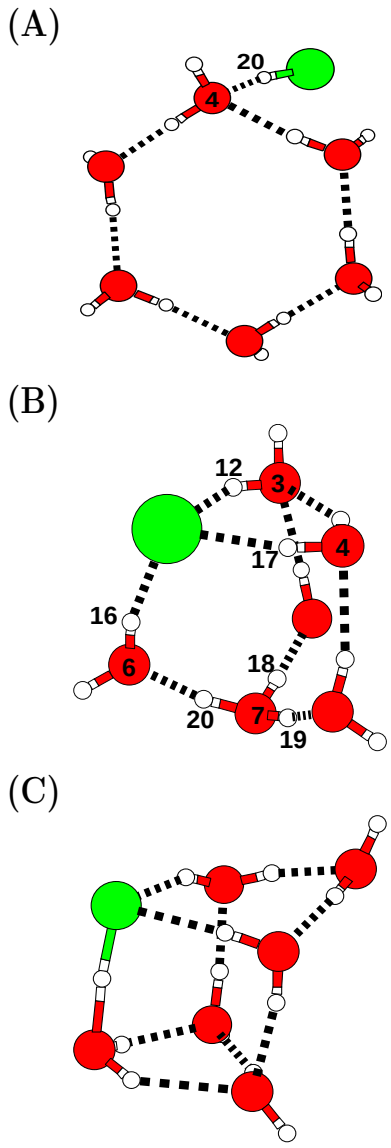

FIG. 1: Representative configurations of the $(H_2O)_6HCl$ clusters. (A) Undissociated ring-like structure; (B) dissociated structure; (C) prism-like structure. H atoms are shown in white, Cl atoms in green (light), and O atoms in red (dark). The dotted lines indicate hydrogen bonds.

we construct two different configurations for $HCl(H_2O)_6$, that fulfill this constraint starting from prism-like geometries, similarly to what was done in Ref. 21.

The configurations obtained after structural optimization at the BLYP level are shown in Fig. 1. All calculations reported in this section are done at the BLYP level of theory. In order to verify the reliability of BLYP calculation, final structures are further optimized with MP2 calculations. Geometrical parameters for the ring-like and dissociated configurations

TABLE I: Selected interatomic distances (in Å) in the ring-like structure (A) determined after BLYP and MP2 optimizations.

	BLYP	MP2
Cl-H20	1.33	1.30
O4–H20	1.79	1.75

TABLE II: Selected interatomic distances (in Å) in the dissociated structure (B) determined after BLYP and MP2 optimizations.

	BLYP	MP2
Cl–H12	2.14	2.02
Cl–H16	2.03	1.99
Cl–H17	2.13	2.23
O7-H18	1.04	1.01
O7-H19	1.04	1.03
O7-H20	1.06	1.03
O6-H16	1.02	0.99
O2–H18	1.55	1.53
O5–H19	1.56	1.47
O6–H20	1.51	1.48

are shown in Tables I and II. For the undissociated ring-like geometry (Fig. 1(A)), we find that in the structure of lowest energy the HCl molecule is hydrogen-bonded through its proton to the water hexamer ($H_2O\cdots HCl$). The H-Cl bond length is 1.33 Å, very close to the equilibrium bond length of gas-phase HCl (the predicted equilibrium bond length of isolated HCl at the same level of theory is 1.30 Å). The length of the $H_2O\cdots HCl$ hydrogen bond is 1.79 Å, in agreement with previous work on undissociated clusters [19, 21, 45]. In the dissociated structure shown in Fig. 1(B) the ion-pair H_3O^+ and Cl^- are embedded in a $(H_2O)_5$ matrix and separated by a water molecule. In this structure, stabilization caused by the proton transfer can be rationalized by the fact that the positive charge on the H_3O^+ disperses through the three hydrogen bonds toward water molecules, forming an Eigen complex ($H_9O_4^+$) [43]. The three $HOH\cdots Cl^-$ hydrogen bonds have lengths of 2.14

TABLE III: Energies of the structures shown in Fig. 1. Energies are in eV and are relative to the lowest energy structure.

structure	BLYP	MP2
A	0.18	0.31
B	0.00	0.00
C	0.36	0.16

Å, 2.13 Å, 2.03 Å(2.02 Å, 1.99 Å, 2.23 Å at the MP2 level), while the hydrogen bonds formed by H_3O^+ with the three surrounding H_2O molecules have an average length of 1.54 Å in BLYP calculations and 1.50 Å in MP2. In the structure shown in Fig. 1(C) the HCl molecule binds to a prism-like water hexamer forming three hydrogen bonds (two acceptors and one donor). The starting configuration of structure (C) consisted of H_3O^+ and Cl^- in close contact, but DFT-BLYP optimization of this structure lead to the displacement of the shared proton towards the Cl^- ion, at a distance of 1.43 Å from Cl^- and 1.41 Å from O, and therefore in proximity of the mid-point between O and Cl. Further MP2 optimization pushes the proton even closer to Cl^- (1.34 Å from Cl^- and 1.58 Å from O), at a distance similar to the one obtained for structure (A), and therefore consistent with the formation of a HCl molecular entity. Such a discrepancy between different levels of theory would in principle deserve further attention, however structure (C) is found to dissociate in the finite temperature runs described in the next section, so we believe this is outside of the scopes of the present work. In summary, the three configurations appear to be representative, at least at the BLYP level of theory, of undissociated (A), fully dissociated (B), and partially dissociated (C) structures.

The energies of the three configurations are reported in Table III both at the BLYP and MP2 level. Even though BLYP and MP2 energy differences for the three $HCl(H_2O)_6$ clusters do not agree for what concerns the ordering of the energy for the structures (A) and (C), both methods find the dissociated structure (B) as the most stable energetically, which confirms that dissociated configurations are energetically preferred in clusters with $n > 4$.

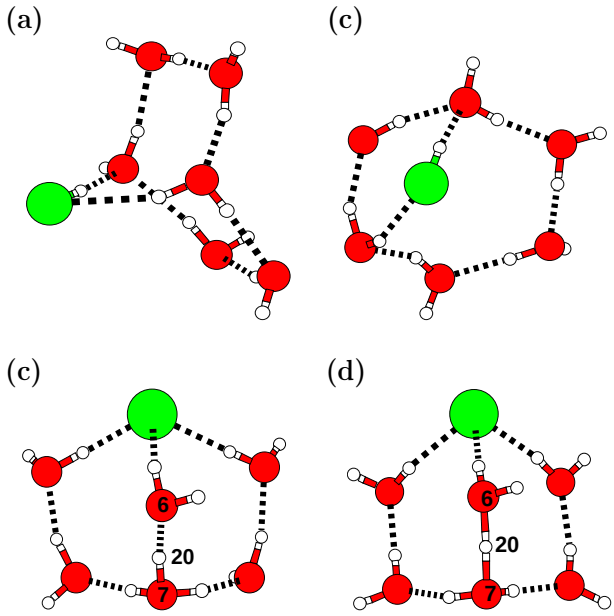

FIG. 2: Snapshots (a) and (b) are taken along the molecular dynamics trajectory at 200 K starting from structure (A). The HCl molecule forms short-lived weak hydrogen bonds with a second water molecule (the Cl···H distance reaches minimum values of about 1.95 Å). Snapshots (c) and (d) are taken along the molecular dynamics trajectory at 200 K starting from structure (B). Snapshot (c) shows an Eigen complex structure and snapshot (d) shows a short-lived asymmetric Zundel structure.

B. Relative cluster stability at atmospheric temperature

The three structures described in Sec. III.A were evolved by Car-Parrinello molecular dynamics at 200 K, a typical temperature in the lower troposphere. The details of the simulation are discussed in Sec. II. Structure (C) is found to dissociate into $(H_2O)_5$+HCl·H_2O when temperature is raised from 120 K to 160 K. Structures (A) and (B) are dynamically stable up to 200 K, within the time scale of the simulation, so the finite-temperature analysis has been carried out on structures (A) and (B) only. Large fluctuations characterize the atomic displacements in both structures. We show in Fig. 2 two snapshots of structure (A) and two of structure (B) taken along the two runs at 200 K. In structure (A) the Cl atom occasionally forms weak temporary bonds with one of the molecules other than the one to which it is permanently bonded as shown in Figs. 2(a) and 2(b). Structure (B) opens up, upon heating, in the "book"-like configuration shown in Fig. 2(c). Further, one of the

protons composing the Eigen complex occasionally moves towards the center of the O-O distance, transforming the Eigen complex into a slightly asymmetric Zundel-like structure (Fig. 2(d)) [11, 43, 44]. Similar short-lived Zundel-like states have been observed in DFT-based simulations of the proton diffusion in bulk water, both at normal density and in the supercritical state [44]. It has been shown that proton diffusion in supercritical water is enhanced with respect to normal water as a consequence of the incomplete and/or hydrogen-bond unsaturated nature of the Eigen complexes. In our clusters, no proton diffusion is observed, in spite of the low-coordination of the hydrogen-bond network. This can be explained by observing that contrary to supercritical water, the solvation shell of the Eigen complex in our cluster is complete.

Based on the above observations, it is clear that thermal fluctuations are far from harmonic in this temperature regime. In order to study the relative stability of our configurations at finite temperature we computed their free energy difference (ΔF) by adding to the average energy difference $\Delta E(T)$ calculated along the two runs at 200 K, the contribution due to their entropy difference ($-T\Delta S$). The entropy difference was evaluated using a vibrational density of states approach [46],

$$S = 3k_B \int_0^\infty D(\omega) \left[x\coth(x) - \log(2\sinh(x))\right] d\omega \ , \tag{2}$$

where $x = \hbar\omega/2k_BT$ and $D(\omega)$ is the vibrational density of states, obtained as the Fourier transform of the time correlation of the atomic velocities. At T= 200 K we obtain for $\Delta E(T) = E_A(T) - E_B(T)$ a value of -0.16 eV, implying that finite temperature effects reverse the sign of the energy contribution to the free energy at 200 K (the value of ΔE for the relaxed structures is +0.18 eV, see Table III). The value of $\Delta E(T)$ calculated within the harmonic approximation is essentially unchanged with respect to the energy difference in the relaxed structures, and is thus significantly different with respect to the value obtained from the molecular dynamics simulation. A possible reason for the discrepancy is the significant structural fluctuations of the two structures (see Fig. 2), and in particular the energetic gain resulting from the formation of the short-lived weak second H-bonds between Cl of the HCl molecule and the water ring in structure (A). Such anharmonic effects are impossible to capture within a harmonic picture of the atomic displacements, and confirm the strong anharmonic nature of the cluster dynamics at 200 K. For $\Delta S(T) = S_A(T) - S_B(T)$ we obtain a value of 0.5×10^{-3} eV/K at 200 K. A calculation of the entropy difference in the harmonic

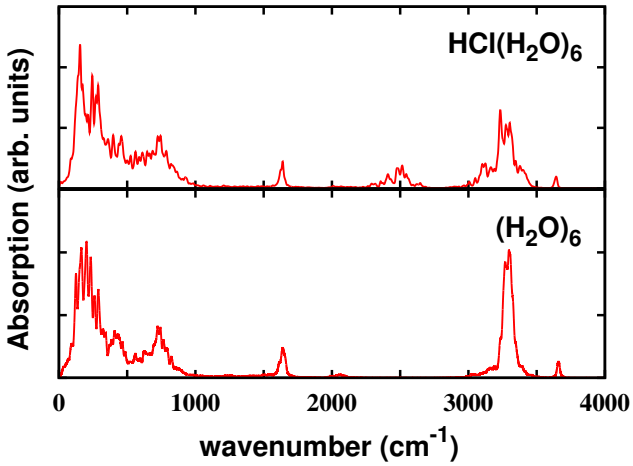

FIG. 3: Top panel: Infrared spectrum of $HCl(H_2O)_6$ in the ring structure (A) at $200K$. The infrared spectrum of the pure $(H_2O)_6$ cluster at 200 K is also shown (bottom panel), for comparison.

limit yields $\Delta S(T) = 0.55 \times 10^{-3}$ eV/K, at the same temperature, in reasonable agreement with the fully anharmonic result obtained with molecular dynamics. Both harmonic and molecular dynamics calculations agree on the fact that the ring isomer has a significantly higher entropy at 200 K, which is consistent with its more open structure. By summing up the contributions from the energy difference $\Delta E(T) = -0.16$ eV and for the entropic contribution to the free energy difference ($-T\Delta S = -0.10$ eV) we obtain a for $\Delta F = F_A - F_B$ at 200 K a value of -0.26 eV, which supports the thermodynamical stability of the ring structure versus the dissociated structure at this temperature. We caution however that a harmonic description of the free energy difference would still give the dissociated structure as more stable at 200 K, though by a smaller amount with respect to the zero temperature results.

C. Infrared spectra at atmospheric temperature

The infrared spectra calculated for the two configurations at 200 K are shown in Figs. 3 and 4, respectively. A comparison of the spectrum of the ring structure (A) with the spectrum calculated for the water hexamer in the ring structure [33], at similar temperature conditions, shows that the peaks above 3000 cm^{-1} are due to the O-H stretches. The small peak at 3700 cm^{-1} is characteristic of "lone", non-hydrogen-bonded O-H units. The peak at

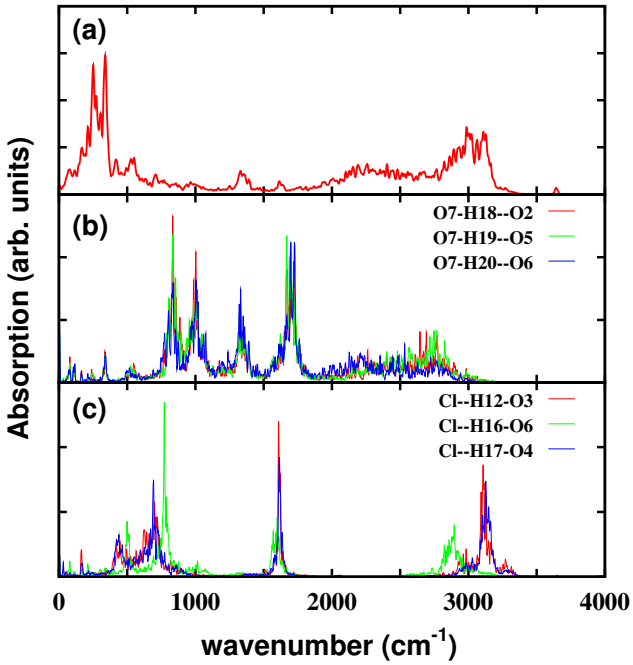

FIG. 4: (a) Infrared spectrum of $Cl^-(H_2O)_5H_3O^+$ in the dissociated structure (B) at $200K$; (b) Vibrational density of states projected on selected atoms in the protonated H_3O^+ unit (see Fig. 1 for atom numbers); (c) Same as (b), but projected on selected atoms surrounding the Cl atom.

1600 cm^{-1} arises from H_2O bending, and the structure below 800 cm^{-1} is due to translational and rotational H_2O modes. HCl contributes with a broad peak at 2500 cm^{-1}, corresponding to the H-Cl stretching vibration. The width is associated with the fluctuating nature of the HCl environment, with Cl occasionally forming a second weak H-bond with a H_2O molecule in the ring, as discussed in Section III.B. The vibrational frequency of the free HCl molecule at the same level of theory is 2800 cm^{-1}, so attachment of HCl to the ring hexamer causes a red-shift of approximately 300 cm^{-1} of this mode, in agreement with earlier calculations [21].

The infrared spectrum of structure (B) has a more complex structure. The peaks at 3700 cm^{-1}, 1600 cm^{-1}, and the continuum below 800 cm^{-1} are similar to those calculated for structure (A), and arise from "lone-OH" stretching, bending, and translational/rotational modes of unprotonated H_2O molecules, respectively. The stretching peak of hydrogen-bonded OH's is broader and slightly red-shifted with respect to that of the ring structure. The broadening arises from the presence of a component coming from the three OH units that are hydrogen bonded to Cl. The vibrational spectrum of such units is clearly seen in Fig. 4(c), where their frequency is found to range between 2800 cm^{-1} to 3200 cm^{-1}. OH

units more strongly bound to Cl (O6-H16 in Fig. 1, see bond lengths to Cl in Table II) display a larger red shift than less weakly bound units (O3-H12, O4-H17). The very broad shoulder between 2000 and 2800 cm^{-1} originates from stretching vibrations of OH units in H_3O^+, as can be argued from the comparison between the infrared spectrum and the vibrational density of states projected on H_3O^+. The three contributions are also broad, but peak on the higher side of the distribution for shorter OH units (O7-H18, O7-H19) and on the lower frequency side for the longer unit (O7-H20), as expected. Moving to lower frequencies, the infrared spectrum of the structure (B) shows then a small peak at 1600 cm^{-1} due, as already said, to bending in intact molecules, and a peak at 1350 cm^{-1} arising from bending modes in H_3O^+, as can be argued by comparison with the vibrational density of states projected on H_3O^+. Finally, the far-infrared portion between 500 and 1000 cm^{-1} is substantially broader and weaker than the corresponding region in the ring structure.

IV. CONCLUSIONS

Our first principle molecular dynamics simulations of the interaction of HCl with water clusters at temperatures comparable to those found in the lower troposphere indicate that the inclusion of temperature effects can modify significantly the results obtained in low-temperature studies. Finite temperatures can alter the thermodynamical stability of different cluster structures by favoring more open conformations, which could in turn hinder the dissociation of the acid. This could explain the discrepancies between theory and experiments reported in the case of HBr [30]. Our simulations also offer a glimpse into the possible effects of temperature in the interpretation of experimental infrared spectra. The large fluctuations experienced by the HCl molecule in the undissociated case gives rise to a significant broadening of its spectroscopic signatures. The dynamical nature of the Eigen-ion band in the dissociated cluster confirms the broad nature of such feature also in a confined geometry [47]. We hope our study will stimulate further efforts to identify spectroscopically larger HCl-water clusters than obtained so far.

V. ACKNOWLEDGMENTS

We acknowledge partial support from INFM/CNR through "Iniziativa per il Calcolo Parallelo" and from MIUR through PRIN No. 2006020543. U. F. T. Ndongmouo and M.-S. Lee acknowledge support from ICTP through the OEA/STEP programme.

---

[1] Solomon, S.; Garcia, R. R.; Rowland, F. S.; Wuebbles, D. J. *Nature* **1986**, *321*, 755.

[2] Molina, M. J.; Tso, T.-L.; Molina, L. T.; Wang, F. C.-Y. *Science* **1987**, *238*, 1253.

[3] McElroy, M. B.; Salawitch, R. J. *Science* **1989**, *243*, 763.

[4] Brune, W. H.; Anderson, J. G.; Toohey, D. W.; Fahey, D. W.; Kawa, S. R.; Jones, R. L.; McKenna, D. S.; Poole, L. R. *Science* **1991**, *252*, 1260.

[5] Tridico, A. C.; Lakin, M.; Hicks, J. M. In *Laser Techniques in Surface Science*, SPIE Conference Proceedings, SPIE, Bellingham, WA, 1994; Vol. 2125, 160.

[6] Wayne, R. P. *Chemistry of Atmospheres*, 2nd ed. Oxford University Press, New York, 1991.

[7] Nathanson, G.; Davidovitz, P.; Worsnop, D.; Kolb, C. *J. Phys. Chem.* **1996**, *100*, 13007.

[8] *Laboratory Studies of Atmospheric Heterogeneous Chemistry*, Kolb, C. E.; Worsnop, D. R.; Zahniser, M. S.; Davidovitz, P.; Molina, M. J.; Hanson, D. R.; Ravishankara, A. R., Eds.; World Scientific, Singapore, 1995; Vol. 3, pp. 771-875.

[9] Huthweljer, T.; Ammann, M.; Peter, T. *Chem. Rev.* **2006**, *106*, 1375.

[10] Devlin, J. P.; Buch, V.; Mohamed, F.; Parrinello, M. *Chem. Phys. Lett* **2006**, *432*, 462. Buch, V.; Mohamed, F.; Parrinello, M.; Devlin, J. P. *J. Chem. Phys.* **2007**, *126*, 074503.

[11] Botti, A.; Bruni, F.; Ricci, M. A.; Soper, A. K. *J. Chem. Phys.* **2006**, *125*, 014508.

[12] Weimann, M.; Farnik, M; Suhm, M. A. *Phys. Chem. Chem. Phys.* **2002**, *4*, 3933.

[13] Packer, M. J.; Clary, D. C. *J. Phys. Chem.* **1995**, *99*, 14323.

[14] Szczesniak, M. M.; Scheiner, S.; Bouteiller, Y. *J. Chem. Phys.*, **1984**, *81*, 5024.

[15] Latajka, Z.; Scheiner, S. *J. Chem. Phys.* **1987**, *87*, 5928.

[16] Gorb, L. G.; Il'chenko, N. N.; Goncharuk, V. V. *Russ. J. Chem.* **1991**, *65*, 1277.

[17] Chipot, C.; Gorb, L. G.; Rivail, J.-L. *J. Phys. Chem.* **1994**, *98*, 1601.

[18] Lee, C.; Sosa, C.; Planas, M.; Novoa, J. J. *J. Chem. Phys.* **1996**, *104*, 7081.

[19] Re, S.; Osamura, Y.; Suzuki, Y.; Schaefer III, H. F. *J. Chem. Phys.* **1998**, *109*, 973.

[20] Milet, A.; Struniewiz, C.; Moszynski, R.; Wormer, P. E. *J. Chem. Phys.* **2001** *115*, 349.

[21] Devlin, J. P.; Uras, N.; Sadlej, J.; Buch, V. *Nature* **2002**, *417*, 269.

[22] Bussolin, G.; Casassa, S.; Pisani, C.; Ugliengo, P. *J. Chem. Phys.* **1998**, *108*, 9516.

[23] Al-Halabi, A.; Kleyn, A. W.; Kroes, G. J. *Chem. Phys. Lett.* **1999**, *307*, 505.

[24] Isakson, M. J.; Sitz, G. O. *J. Phys. Chem. A* **1999**, *103*, 2044.

[25] Kroes, G. J.; Clary, D. C. *J. Phys. Chem.* **1992**, *96*, 7079.

[26] Wang, L.; Clary, D. C. *J. Chem. Phys.* **1996**, *104*, 5663.

[27] Ando, K.; Hynes, J. T. *J. Phys. Chem. B* **1997**, *101*, 10464.

[28] Hurley, S. M.; Dermota, T. E.; Hydutsky, D. P.; Castleman, Jr., A. W. *J. Chem. Phys.* **2003**, *118*, 9272.

[29] Conley, C.; Tao, F.-M. *Chem. Phys. Lett.* **1999**, *301*, 29.

[30] Voegele A. F.; Liedl, K. L. *Angew. Chem. Int. Ed.* **2003**, *42*, 2114.

[31] Smith, A.; Vincent M. A.; Hillier, I. H. *J. Phys. Chem. A*, **1999**, *103*, 1132.

[32] Rodriguez, J.; Laria, D.; Marceca, E. J.; Estrin, D. A. *J. Chem. Phys.* **1999**, *110*, 9039.

[33] Lee, M.-S.; Baletto, F.; Kanhere, D. G.; Scandolo, S. to be submitted.

[34] Xantheas, S. S. *J. Chem. Phys.* **1994**, *102*, 4505.

[35] Troullier, N.; Martins, J. L. *Phys. Rev. B* **1991**, *43*, 1993.

[36] Sprik, M.; Hutter, J.; Parrinello, M. *J. Chem. Phys.* **1996**, *105*, 1142.

[37] www.quantum-espresso.org

[38] Frisch, M. J.; Trucks, G. W.; Schlegel, H. B.; Scuseria, G. E.; Robb, M. A.; Cheeseman, J. R.; Montgomery, J. A.; Vreven, Jr., T.; Kudin, K. N.; Burant, J. C.; Millam, J. M.; Iyengar, S. S.; Tomasi, J.; Barone, V.; Mennucci, B.; Cossi, M.; Scalmani, G.; Rega, N.; Petersson, G. A.; Nakatsuji, H.; Hada, M.; Ehara, M.; Toyota, K.; Fukuda, R.; Hasegawa, J.; Ishida, M.; Nakajima, T.; Honda, Y.; Kitao, O.; Nakai, H.; Klene, M.; Li, X.; Knox, J. E.; Hratchian, H. P.; Cross, J. B.; Adamo, C.; Jaramillo, J.; Gomperts, R.; Stratmann, R. E.; Yazyev, O.; Austin, A. J.; Cammi, R.; Pomelli, C.; Ochterski, J. W.; Ayala, P. Y.; Morokuma, K.; Voth, G. A.; Salvador, P.; Dannenberg, J. J.; Zakrzewski, V. G.; Dapprich, S.; Daniels, A. D.; Strain, M. C.; Farkas, O.; Malick, D. K.; Rabuck, A. D.; Raghavachari, K.; Foresman, J. B.; Ortiz, J. V.; Cui, Q.; Baboul, A. G.; Clifford, S.; Cioslowski, J.; Stefanov, B. B.; Liu, G.; Liashenko, A.; Piskorz, P.; Komaromi, I.; Martin, R. L.; Fox, D. J.; Keith, T.; Al-Laham, M. A.; Peng, C. Y.; Nanayakkara, A.; Challacombe, M.; Gill, P. M. W.; Johnson, B.; Chen, W.; Wong, M.

W.; Gonzalez, C.; Pople, J. A. Gaussian 03, Revision B.04; Gaussian, Inc., Pittsburgh PA, 2003.

[39] Car, R.; Parrinello, M. *Phys. Rev. Lett.* **1985**, *55*, 2471.

[40] Grossman, J. C.; Schwegler, E.; Draeger, E. W.; Gygi, F.; Galli, G. *J. Chem. Phys.* **2004**, *120*, 300. Schwegler, E.; Grossman, J. C.; E. W.; Gygi, F.; Galli, G. *J. Chem. Phys.* **2004**, *121*, 5400.

[41] Silvestrelli, P. L.; Bernasconi, M.; Parrinello, M. *Chem. Phys. Lett.* **1997**, *277*, 478.

[42] Liu, K.; Brown, M. G.; Carter, C.; Saykally, R. J.; Gregory, J. K.; Clary, D. C. *Nature* **1996**, *381*, 501. Gregory, J. K.; Clary, D. C.; Liu, K.; Brown, M. G.; Saykally, R. J. *Science* **1997**, *275*, 814.

[43] Marx, D.; Tuckerman, M. E.; Hutter, J.; Parrinello, M. *Nature* **1999**, *397*, 601. Tuckerman, M.; Laasonen, K.; Sprik, M.; Parrinello, M. *J. Chem. Phys.* **1995**, *103*, 150.

[44] Boero, M.; Ikeshoji, T.; Terakura, K. **ChemPhysChem 2005**, *6*, 1775.

[45] Bacelo, D. E.; Binning Jr., R. C.; Ishikawa, Y. *J. Phys. Chem. A* **1999**, *103*, 4631.

[46] de Sousa, R. L.; Leite Alves H. W. *Braz. J. Phys.*, **2005**, *36*, 501.

[47] Headrick, J. M.; Diken, E. G.; Walters, R. S.; Hammer, N. I.; Christie, R. A.; Evgeniy, J. C.; Myshakin, E. M.; Duncan, M. A.; Johnson, M. A.; Jordan, K. D. *Science* **2005**, *308*, 1765.